Results in Engineering 26 (2025) 104828

Contents lists available at ScienceDirect

Results in Engineering

journal homepage: www.sciencedirect.com/journal/results-in-engineering

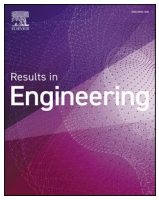

Research paper

Electrochemical separation of chromium/collagen from wet blue in a single step: recycling of tannery waste to promote a circular economy

Croswel E. Aguilar Quiroz [a,*], Yanet Guevara Ruiz [a], Javier F. Urquiaga Rios [a], Eymi G. Layza Escobar [a], Marco A. Siqueira Rodrigues [b]

[a] Laboratorio de Catálisis Adsorbentes y Materiales, Grupo de Investigación en Energía Medioambiente y Tecnología, Universidad Nacional de Trujillo, Peru
[b] Laboratório Aquário, Feevale Universitária, Brazil

ARTICLE INFO

Keywords:
NaOH
NaCl electrolysis
Collagen
Cr^{3+}
Alkaline hydrolysis

ABSTRACT

The leather industry produces tons of solid waste containing significant amounts of chromium. Without any safe deposition, these can potentially pollute the environment. This article develops an electrochemical method to remove chromium and separate collagen from wet blue chromium shaving (WBCS). The raw WBCS had an initial content of 28.5 g Cr^{3+}/Kg. The process was carried out in a three-compartment electrochemical reactor assembled with cationic membranes, using graphite and titanium as electrodes. The single-stage process produces NaOH by electrolysis of NaCl solution, while OH- hydrolyzes the collagen from WBCS in situ. The influence of NaCl concentration 1–10 g/L, reaction time 0.5 - 5 h, temperature 60 - 99 °C, and current density were studied. The products were analyzed using FTIR, UV–vis spectrophotometry and TGA. NaOH was generated proportional to NaCl concentration and current density. WBCS hydrolysis varied with OH^- concentration, temperature, and time. The conditions to achieve the highest chrome-collagen separation were 5 g NaCl/L, pH 11.7, 0.31 A/cm^2, 90 °C, during 1 - 2 h of reaction. Chromium precipitates as amorphous $Cr(OH)_3$ at a pH higher than 10, while collagen remains in the aqueous phase. Over 99 % of Cr^{3+} extraction from WBCS was achieved. An analysis of the process sustainability was made for byproducts reuse in the tannery.

1. Introduction

WBCS represent 25 % of the total solid waste produced by the tanning industry, which needs special disposal due to adsorbed contaminants within [1,2]. A critical issue in WBCS is its chromium content, which can convert its oxidation state from Cr^{3+} to Cr^{6+}. The last can be formed by oxidation during incineration in landfills [3] or by contact with manganese oxide minerals at room conditions [4]. In living beings, Cr^{6+} is highly toxic and causes severe health damage: lung or stomach cancer, bladder disorders, gastrointestinal ulcers, DNA damage, dermatitis, and pneumonia [5]. In the environment, Cr^{6+} can easily accumulate in the ground and aquifers due to its high solubility, where crops and livestock are exposed [6,7]. Both scenarios represent high risks that need to be addressed.

Diverse technologies focus on WBCS recycling and integration into the circular economy, such as biogas production [8], carbon aerogels [9], adhesives [10], nanomaterials [11], biochar [12], biofuels [13], adsorbents [14], bricks [15], etc. However, these technologies don't consider the chromium content and its conversion into Cr^{6+}. The chromium separation from collagen in WBCS is based on breaking the Cr-O bond formed by the carboxylic groups of fibrillar collagen type I cross-linked to Cr^{3+}, as shown in Fig. 1 [16].

Standard technologies for Cr-collagen separation are ultrasound, thermal processes, acid, enzymatic, and alkaline hydrolysis. Ultrasound separation has reported Cr removal around 71 – 98 % [17,18], but a second stage is needed. Thermal processes recover chromium oxide at temperatures near 850 °C but decompose collagen into CO_2 and other contaminants [19]. Separation by hydrolysis requires chemical reagents like acids, alkalis, specific enzymes, and resins. Acid hydrolysis with acetic acid (2 M) can hydrolyze 87 % collagen in 6 h at 80 °C [20]; sulfuric acid separates 35–60 % of Cr^{3+}, 40 °C in up to 6 days [21], and addition of cation exchange resin removes 95 % of Cr [22]. Alkaline hydrolysis with NaOH (0.47 M) recovered 87 % collagen at 70 °C in 1.5 h [23], the maximum collagen hydrolysis 69.8 %, 59.8 % and 68 % was reached with 7 % NaOH, 10 % MgO, and 10 % CaO respectively at 98 °C [24], 30 % NH_4OH hydrolyzed 55.6 % of the protein at 120 °C during 6 h

* Corresponding author.
E-mail address: caguilar@unitru.edu.pe (C.E. Aguilar Quiroz).

https://doi.org/10.1016/j.rineng.2025.104828
Received 20 February 2025; Received in revised form 26 March 2025; Accepted 5 April 2025
Available online 5 April 2025

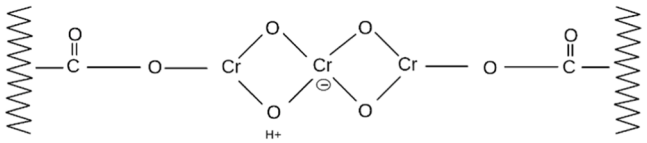

Fig. 1. Chrome complexes with the protein carboxyl groups. From Elshahat H. A. Nashy et al. [16].

[25]. Thus, conventional hydrolysis separation requires concentrated chemical agents, high reaction times, temperatures, and pressures.

Combining hydrolysis with electrochemistry can improve and accelerate the process. Electrolysis involves applying the electric field to dissociate water into OH^- and H^+ ions under atmospheric conditions. In this sense, NaCl can provide Na^+ ions for the formation of NaOH and contribute to ionic mobility for water dissociation. The use of membrane in electrolysis allows the selective dissociation and transport of ions and radicals, which can be used to optimize chemical reactions. Cationic membranes direct OH^- in the production of NaOH by brine electrolysis, such as in chlor-alkali, porous diaphragm, electrodialysis, and direct electrosynthesis processes [26]. The generation of Na^+, Cl^- and OH^- with cation exchange membranes occurs by the reactions [26,27]:

Anode

$$2Cl^- \rightarrow Cl_2 + 2e^- \quad (1)$$

Cathode

$$2H_2O + 2e^- \rightarrow H_2 + 2OH^- \quad (2)$$

General reaction

$$2NaCl + 2H_2O \rightarrow Cl_2 + H_2 + 2NaOH \quad (3)$$

The NaOH supply and handling can limit the operation and economy of processes like alkaline hydrolysis in tanneries, where an electrochemical production of NaOH and hydrolysis of WBSC separately are required.

This work aims to separate chromium and collagen from WBCS by a single-stage electrochemical intensification process, combining electrolytic generation of OH^- ions with in situ hydrolysis of WBCS. The system consists of a three-chamber electrolytic cell: two anodic chambers filled with NaCl solution and a cathodic (central) chamber containing the WBCS. OH^- ions generated by brine electrolysis hydrolyze WBCS in the cathodic cell, separating the collagen and precipitating chromium. The influence of variables such as NaCl concentration, reaction time, and current density are investigated.

The proposed method for WBCS treatment aims to reduce waste generation and disposal costs with the safe recycling of collagen and chromium. The products and byproducts of the process tend to be reused: hydrolyzed collagen in the aqueous phase can be used in food, cosmetics, fertilizer, among others; separated chromium can be recycled in leather production by acid activation; and reuse of NaCl from skin preservation can also be possible; minimizing environmental pollution and fomenting a circular economy.

2. Materials and methods

2.1. Reagents

Raw WBCS was given by Ecologica del Norte E.I.R.L. tannery. Trujillo-Peru. Commercial-grade NaCl was used. Diphenylcarbazide reagent for Cr^{6+} identification was made with Marechey-Nagel NanoColor Chromate Kit. The oxidation of Cr^{3+} to Cr^{6+} was carried out using NanOx Metal from Marechey-Nagel.

2.2. Equipment

The reactor was made of polyethylene and had three compartments of 500 mL each: two anodic (external) and one cathodic cell (central). They are connected by cationic membranes (CEM) type HDX-100, with ion exchange capacity ≥ 2.0 mol/kg (dry), permselectivity ≥ 90 %, water permeability ≤ 0.1 mL/h.cm^2 and surface resistance ≤ 20 ohm.

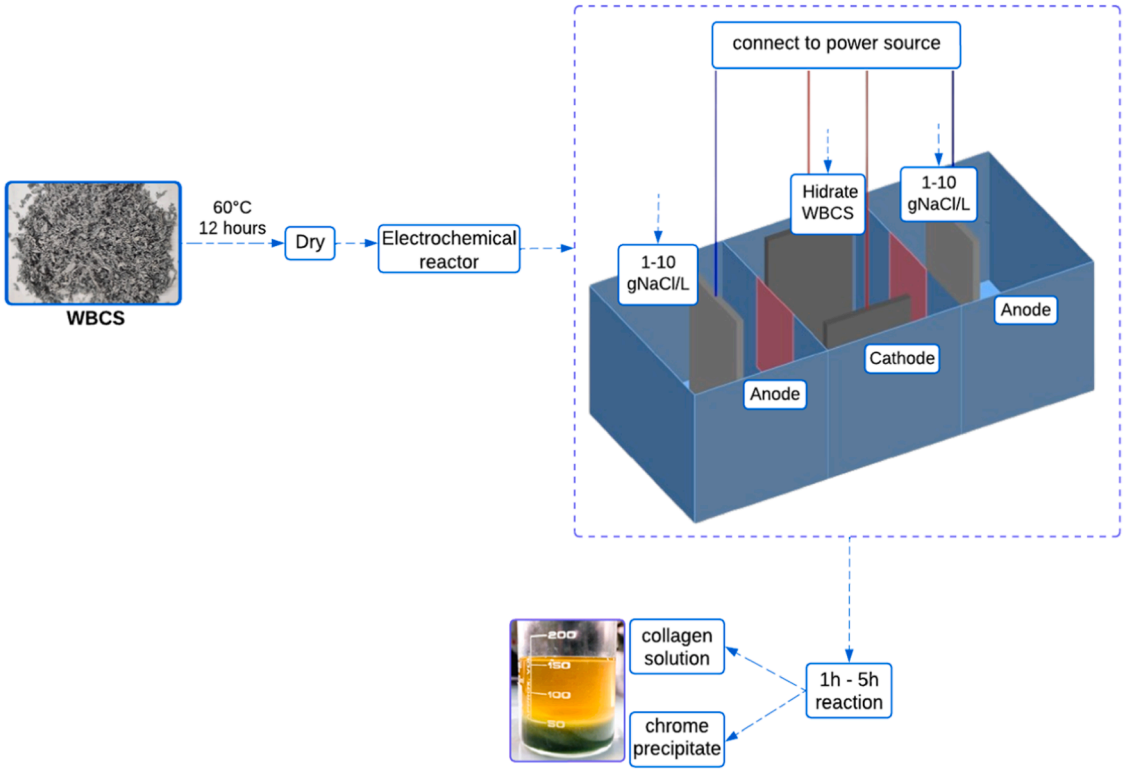

Fig. 2. Process scheme of the electrolytic treatment of WBCS for chrome-collagen separation.

Table 1
Leached Cr^{3+} (%) in the aqueous phase or precipitate, temperature, and pH solution.

Time (Hours)	1 g NaCl/L				2.5 g NaCl/L				5 g NaCl/L				10 g NaCl/L			
	T (°C)	pH	% Cr		T (°C)	pH	% Cr		T (°C)	pH	% Cr		T (°C)	pH	% Cr	
			S	SD*			S	SD*			P	SD*			P	SD*
0.5	42	3.9	0.9	0.45	53	4.1	1.2	0.15	66	10	98.3	1.15	80	12	99.7	0.74
1	62	4.4	3.1	0.56	77	6.1	2.8	0.21	90	12	99.5	0.58	99	12	99.8	0.62
2	64	5.6	5.7	0.4	78	9.1	4.3	0.25	92	12	99.1	2.52	98	13	99.9	0.83
3	65	6.4	7	0.46	80	9.2	8.5	0.36	92	12	99.9	1.53	99	13	99.8	0.84
4	59	6.5	8.2	0.67	79	9.5	16	0.15	85	12	99.9	2.65	97	13	99.5	0.66
5	60	6.5	16	0.36	80	9.6	31	0.87	90	12	99.8	1.29	98	13	99.9	2.54

S* Cr^{3+} in aqueous solution.
P* precipitated chromium.
SD* Standard deviation.

cm^2. The electrodes are two graphite plates of 18 cm^2 area in cathodic compartments and two $Ti/_{0.7}TiO_2/_{0.3}RuO_2$ plates of 18 cm^2 area in anodic compartments. In the reactor set up, NaCl solution was introduced into the anodic compartment to undergo the electrolytic decomposition, while hydrated WBCS were in the cathodic compartment for chrome-collagen separation.

2.3. Procedure

WBCS in sizes ± 2 mm were dried at 60 °C for 12 h. Subsequently, 20 g of WBCS was hydrated in 300 ml H_2O for 12 h, and then placed in the cathodic compartment with graphite electrodes. The anode compartments hold 450 ml of NaCl solution at 1 to 10 g/L besides $Ti/_{0.7}TiO_2/_{0.3}RuO_2$ electrodes. For the reactor operation, 50 V in DC current was supplied to the electrodes connected in parallel. The amperage was adjusted based on the NaCl concentration to further enhance the reactor's efficiency: the average current density used for each solution of 1, 2.5, 5 and 10 g NaCl/L were 0.1762, 0.2376, 0.2861 and 0.3136 mA/cm^2 respectively. Reaction times went from 0.5 to 5 h. Aliquots were extracted to analyze Cr^{3+}, NaOH, HCl, and collagen. Likewise, pH and conductivity are measured in the system (Fig. 2). The chlorine gas produced in the anode compartments was passed through a NaOH solution to generate bleach (NaClO).

2.4. Analysis

The concentrations of NaOH and HCl produced in the system compartments were measured by ASTM E200–19 titration with CH_3COOH (0.01 M - 0.1 M) and NaOH (0.01 M - 0.1 M) respectively. Quantification analysis of Cr^{3+} was performed by the spectrophotometric method using the diphenylcarbazide reagent in the Orion AquaMate 8000 UV–Vis Spectrophotometer at 540 nm. Cr^{6+} content was determined using the diphenylcarbazide reagent. For Cr^{3+} quantification, a total oxidation of Cr^{3+} to Cr^{6+} was carried out using NanOx Metal. The quantity of Cr^{3+} corresponds to the difference between the initial Cr^{6+} and the Cr^{6+} obtained by total oxidation. Cr^{3+} in WBCS was quantified by acid digestion with H_2SO_4. The tests were performed in triplicate. The Fourier Transform Infrared Spectrometer with Universal Attenuated Total Reflection Sampling Accessory (ATR-FTIR) identified the functional groups (Perkin-Elmer®, Spectrum TWO). TGA /DTG Thermogravimetric Analysis of collagen and WBCS was done at Balance Netzsch 409 PC for high temperatures (up to 1500 °C) with controlled atmosphere and data acquisition software. Nitrogen flow was 50 mL/min, and the heating speed was 10 °C/min. Data analysis for kinetics was done using Curve Table 2D software. The results were statistically treated with Statgraphics Centurion 17.

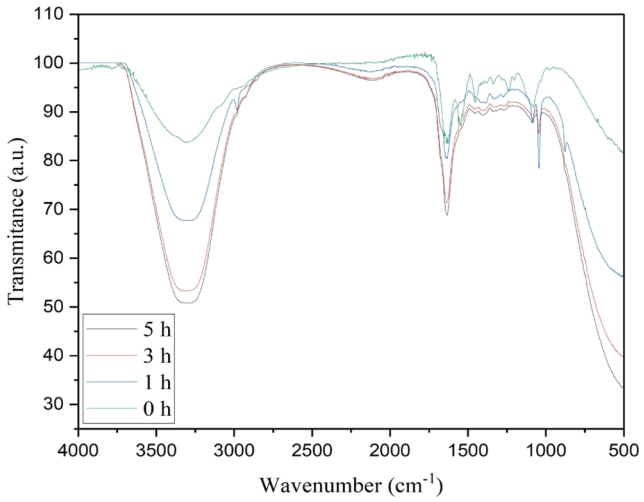

Fig. 3. FTIR of initial WBCS and collagen gel obtained of the system with 5 g NaCl/L after 1, 3, and 5 h of reaction.

3. Results and discussion

3.1. Characterization

WBCS had 2.9 % of Cr^{3+} content, the Cr^{6+} wasn't detected. The XRD analysis of the precipitates corresponding to the tests with 1, 2.5, 5, and 10 g NaCl/L didn't present signals corresponding to crystalline structures but rather a lot of noise from amorphous structures [28]. The chemical analysis of these precipitates (Table 1) shows that they are Cr^{3+}, possibly as $Cr(OH)_3$.

Chrome-collagen separation occurred in the cathodic compartment, $Cr(OH)_3$ was precipitated while the supernatant collagen was separated and analyzed by ATR-FTIR (Fig. 3). The characteristic bands for the collagen separated with 5 g NaCl/L and reaction times of 1, 3, and 5 h are presented. Unhydrolyzed WBCS collagen was designated as 0 h. The broad band at 3300 cm^{-1}, corresponding to the N—H bond of amide A of the peptides [29,30], was present in all samples and was more intense for the collagen obtained after 3 and 5 h of reaction. A relatively weak band at 2962 cm^{-1} was observed in all samples, corresponding to the CH_2 bond of amide B [31], except for the 1 h sample, where the signal was intense. The amide I identified by the $C=O$ band at 1640 cm^{-1} [31, 32] was present in all samples. The band at 1548 cm^{-1} of amide II [32, 33] and the peaks at 1450/1272 cm^{-1} points out the presence of the triple-helix structure [34,35]; these bands are present in the raw WBCS and vanish in the collagen obtained by hydrolysis (1, 2.5, and 5 h) indicating that there is collagen degradation. C—O—C bonds at 1080 cm-1 [33] were also present in all samples. The new band appearing in the collagen samples after 1, 3, and 5 h of reaction is the C—O bond at

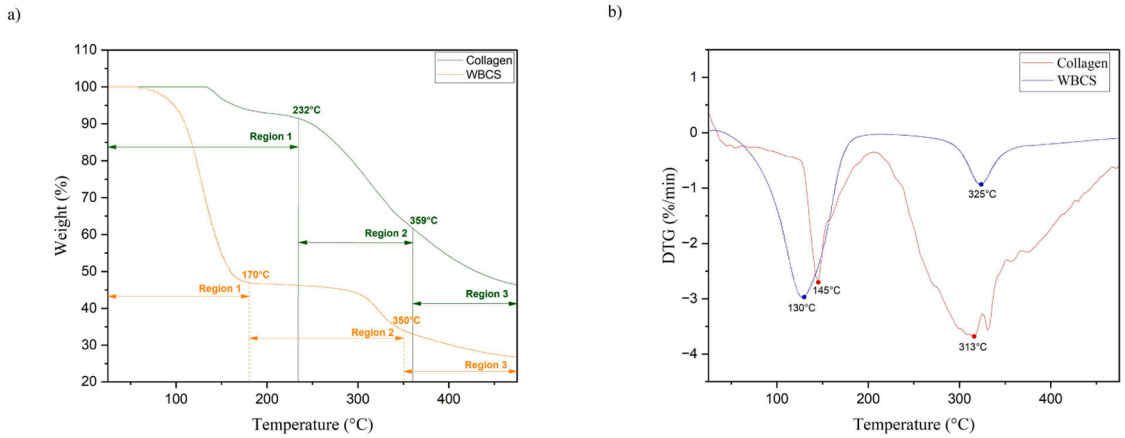

Fig. 4. TGA **(a)** and DTG **(b)** of collagen were obtained after 5 h of reaction and with 5 g NaCl/L.

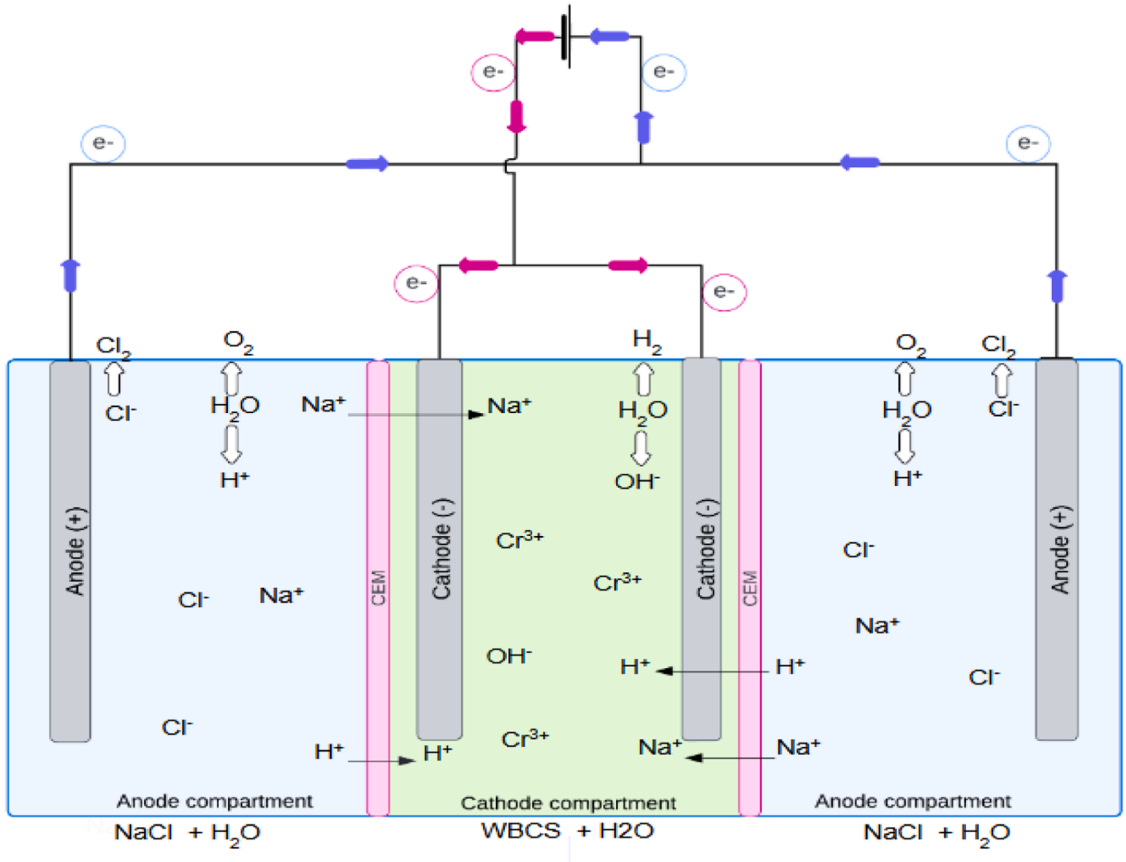

Fig. 5. Diagram of the membrane reactor of NaOH production for in-situ hydrolysis.

1039 cm^{-1} [33] corresponding to carbohydrate moieties. In summary, the collagen structure separated by hydrolysis was partially degraded in relation to the collagen in the WBCS.

From the TGA/DTG analysis (Fig. 4a), it can be observed in the range from 25 to 232 °C, that the collagen weight lost 9 % weight mainly due to water and some fractions of unconsolidated collagen. In contrast, the WBCS that was hydrated before the process had a more significant loss of 53 % up to 170 °C, corresponding to the water found on its surface. In the following range, from 170 to 350 °C, 14 % of the weight of WBCS was lost due to the elimination of structural water, amino groups, decarboxylation, and decomposition of volatile compounds [36,37]. Cr^{3+}in the WBCS gives collagen more structural stability at 350 °C. At higher temperatures, the collagen continues to degrade. In Fig. 4b, the weight loss rate in the first stage (up to 145 °C) corresponds mainly to surface water. It reaches its maximum value at 130 °C for WBCS and 145 °C for collagen. At this stage, collagen, having a lower water concentration on its surface, presents relatively more thermal-resistance than WBCS. At higher temperatures, collagen begins to degrade at 200 °C, reaching the highest rate at 313 °C. In contrast, WBCS begins to degrade at 300 °C, reaching the highest rate at 325 °C. The presence of Cr^{3+} in WBCS confers more thermal stability than collagen; therefore, the rate of thermal degradation is lower with increasing temperature.

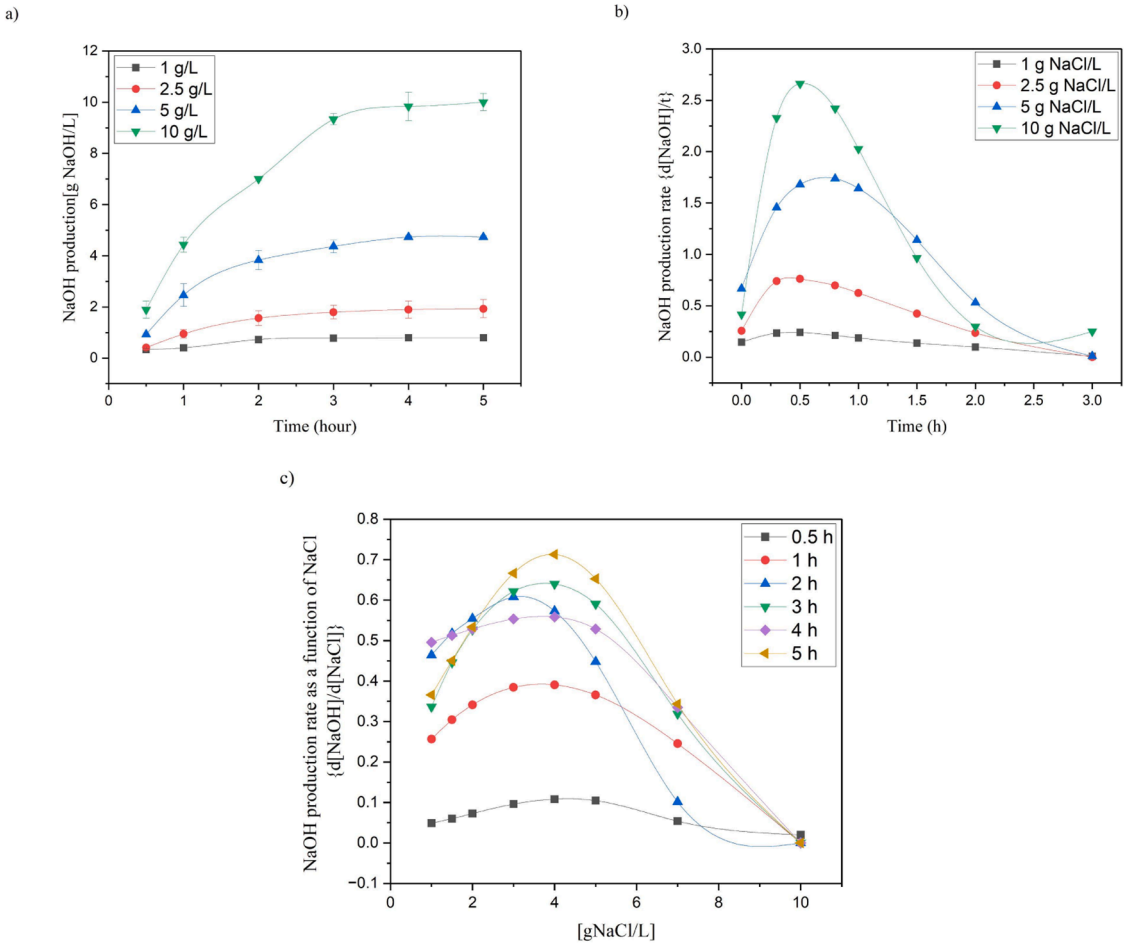

Fig. 6. a). NaOH production as a function of NaCl concentration without adding WBCS b) NaOH production rate as a function of time and NaCl concentration without adding WBCS c) NaOH production rate as a function of NaCl concentration in the reactor, without adding WBCS.

3.2. NaOH production in the electrochemical reactor

NaOH production (without the presence of WBCS)

During the electrolysis of NaCl and H_2O in the membrane reactor (Fig. 5), the H^+ and Na^+ ions electro-migrate towards the cathode compartment, forming H_2 and NaOH with the OH^- generated by electrolysis of H_2O, respectively [27]. Cl^- ions react to form HCl; Cl_2 is produced on the surface of the titanium anode, and H_2 on the surface of the graphite electrode according to reactions (1), (2) and, (3).

Fig. 6a shows the behavior of sodium hydroxide production as a function of reaction time and sodium chloride concentration. In this process, WBCS were not added. The increase of NaCl concentration and time promotes an increase in sodium hydroxide formation. NaOH production was proportional to NaCl concentrations up to 5 g NaCl/L during the first 2 h of reaction. After 2 h, equilibrium was reached due to NaCl depletion and lack of mobility, less Na^+ ions migrating from anodic to cathodic compartment to form NaOH. However, the electrolysis of H_2O continues over time, and when 10 g NaCl/L is added, NaOH generation grows exponentially up to 3 h due to the increase in ionic mobility [38] and then linearly up to 5 h.

The NaOH formation rates (dNaOH/dt) over time exhibit a Gaussian behavior (Fig. 6b) proportional to the NaCl concentration. The maximum production rates at 0.5 h of NaOH were 0.006, 0.019, 0.042, 0.066 (moles NaOH/L*h) for 1, 2.5, 5 and 10 g NaCl/L respectively. After 3 h, it decreased to zero except at 10 g NaCl/L, which changes to linear at 2 h. The production rate of NaOH in the time up to 2 h of reaction was of the type:

$$\frac{d[NaOH]}{dt} = a\, e^{(-0.5(t-0.64)/0.37)^2}$$

Where a has values of 1.12, 2.05 and 3.5 for 1, 2.5 and 5 g NaCl/L respectively. These values are proportional to the dissociation of NaCl into Na^+ and Cl^- ions, which increases the ionic mobility. Therefore, the transfer of ions and electrons increases the reaction rate at higher NaCl concentration. Also, for the range of NaCl concentrations studied, only 2 h of reaction were required to form maximum amounts of NaOH, but the highest conversion of NaOH was reached in one hour. Thus, the hydrolysis reaction of WBCS occurs mainly in a two-hour reaction.

The influence of NaCl concentration in NaOH formation rate (Fig. 6c) was a Gaussian function. Regardless of the reaction time, the highest NaOH production rate is between 3 and 5 g/L of NaCl, with the optimal amount being 4 g/L. It is observed that higher NaCl concentrations decrease the NaOH production rate. While it is known that increasing the NaCl concentration increases the ionic conductivity in the system, and therefore, the electrochemical reaction rate. However, for relatively high NaCl concentrations, the OH^- and Cl^- co-ions increase strongly, and a part of them moves Cl^- toward the cathode and OH^- to the anode, which generates a drop in electrical efficiency [39,40]. Consequently, the hydrolysis of WBCS can be carried out in the first two hours of the reaction using <5 g/L NaCl concentrations.

3.3. Hydrolysis of WBCS

3.3.1. NaOH consumption

WBCS was added in the cathodic compartment where the NaOH was

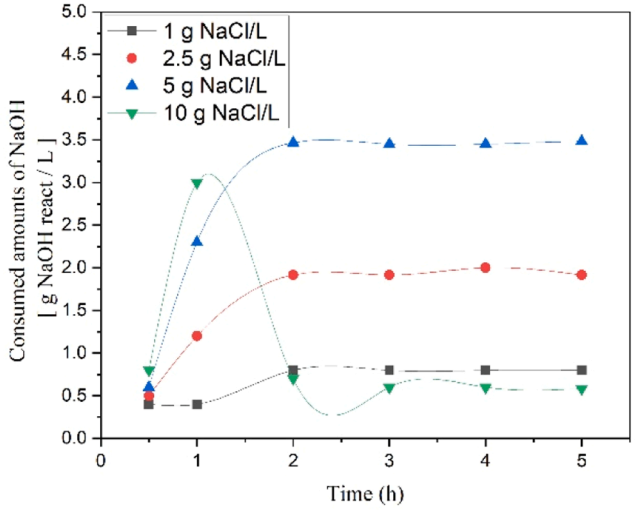

Fig. 7. Consumed amounts of NaOH in the WBCS hydrolysis for different NaCl concentrations in the system.

generated by the electromigration of Na^+ (Eq. 1 to 2). The ions OH^- of NaOH reacted in the reactor with the WBCS to break the collagen-chromium bond, separating both compounds, while Cr^{3+} precipitated as $Cr(OH)_3$ at a very basic pH [41]. As the OH^- concentration system reaction was proportional to NaOH concentration, the OH^- reaction continued in the NaOH concentration's function and the system's pH. Fig. 7 shows the NaOH (g/L) that reacts to hydrolyze the WBCS, which corresponds to the difference between the NaOH produced without and with WBCS in the reactor (eq. 4) for different times and NaCl concentrations.

$$NaOH_{(reacts)} = NaOH_{(produced\ without\ WBCS)} - NaOH_{(produced\ with\ WBCS)} \quad (4)$$

For 1 g NaCl/L, the WBCS hydrolysis occurs in the first 2 h, reacting 0.8 g NaOH/L generated. The pH (Table 1) in the cathodic compartment increased from 3.6 (0 h) to 6.5 (3 h) due to the hydrolysis reaction of the WBCS, stabilizing at pH 6.5, reaching the hydrolysis equilibrium. When 2.5 g NaCl/L was added, only 1.9 g NaOH/L reacted in the first two hours, leaving ± 0.1 g NaOH/L unreacted. The system's pH increased to 9.0 at 2 h and remained constant over time. However, for 5 g NaCl/L, total hydrolysis occurs in the first hour, with 3.5 g NaOH/L reacting to reach pH 11.7. Similar values are obtained for 10 g NaCl/L. These results show that the hydrolysis of the WBCS took place simultaneously with the generation of NaOH in the first 2 h of reaction and it is independent of the amount of NaCl added. Therefore, the consumption of NaOH over time is a parameter that indicates the degree of reaction.

3.3.2. *Extraction of Cr^{3+}*

The OH^- ions generated in the reactor breaks Cr-collagen and Cr-Cr covalent bonds in the WBCS structure [20,43], releasing the Cr^{3+} and collagen into the aqueous phase (Fig. 8).

The separated Cr^{3+} remains in the aqueous phase or precipitates as $Cr(OH)_3$, mainly depending on the pH, initial NaCl concentration, and temperature, as observed in Table 1 and Fig. 9. When NaCl wasn't added, the Cr^{3+} extraction in aqueous phase was 152.7 mg Cr^{3+}/L (3 h), which remained constant over time, and the solution reached pH=5.3. In this case, NaOH required for hydrolysis was provided by the residual NaCl inside WBCS structure, which is added to the skins before tanning [3].

When 1 g NaCl/L was added, the Cr^{3+} extraction to the aqueous phase increased linearly over time up to 157.4 mg Cr^{3+}/L in 3 h, and after 5 h exponentially reached 308 mgCr^{3+}/L at pH=6.5. For 2.5 g NaCl/L added, the extraction of Cr^{3+} was exponential, reaching 598 mg Cr^{3+}/L at 5 h and pH=9.6. A green aqueous phase was observed in the cathodic compartment where Cr^{3+} was in solution. In $Cr(OH)_3$ - H_2O systems, $Cr(OH)_3$ precipitates at a pH greater than 5.5 [42,41,44]. However, Cr^{3+} remains in the aqueous phase even at pH=9.6. In the presence of -OH and -COOH groups of collagen, $Cr(OH)_3$ forms stable and soluble complexes at alkaline pH [45,46]. Likewise, chromium hydroxo complexes $Cr(OH)^{2+}$, $Cr(OH)_2^+$, $Cr(OH)_3^\circ$, and $Cr(OH)_4^-$ are soluble at pH 5.5 – 9 [47]. These $Cr(OH)_3$ intermediates and precursors could affect Cr^{3+} precipitation when pH ⟨ 10, like in the 2.5 g NaCl/L essay, where it remains in solution with collagen. However, pH ⟩ 10.5 exhibited higher $Cr(OH)_3$ precipitations (99 %) at 5 and 10 g NaCl/L; under these conditions, those complexes don't affect Cr^{3+} precipitation.

After 0.5 h of reaction at 5 or 10 g NaCl/L concentrations, only 0.4 % and 0.1 % of Cr^{3+} was detected in the aqueous solution, and >98 % were precipitated at pH 10.4 and 11.5, respectively. After 1 h of reaction, >99.5 % chrome was precipitated, and no Cr^{3+} was detected in the aqueous solution, conditions that remained constant until 5 h. In these cases, a defined formation of two phases was observed: an upper, yellow aqueous phase corresponding to collagen and a lower, greenish phase

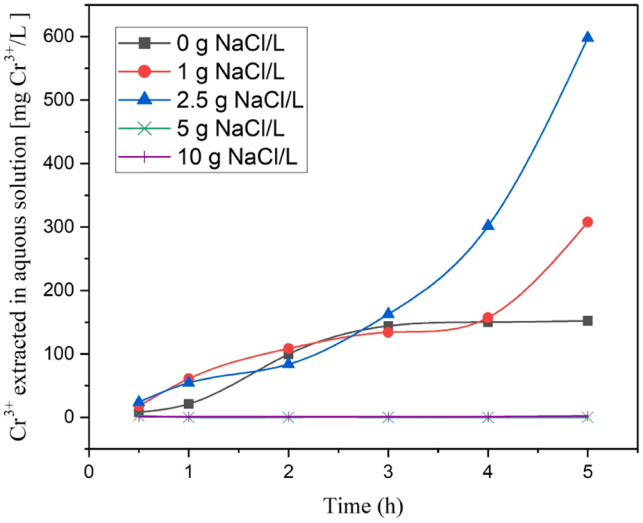

Fig. 9. Cr^{3+} extraction toward aqueous solution by hydrolysis of WBCS in function of time, at 0–10 g NaCl/L addition.

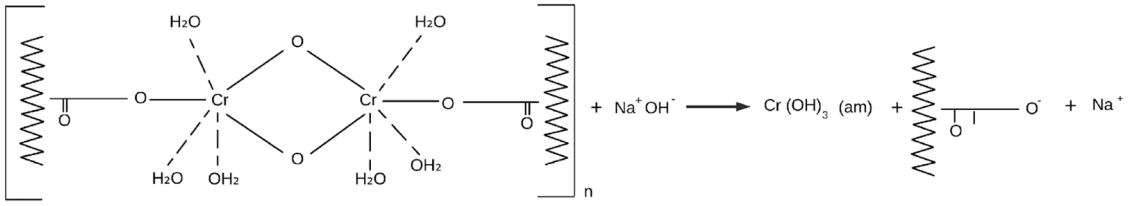

Chromium and collagen complex (WBCS)

Fig. 8. Hydrolysis of WBCS with OH^- to release $Cr(OH)_3$ and collagen. Note. Adapted from [22].

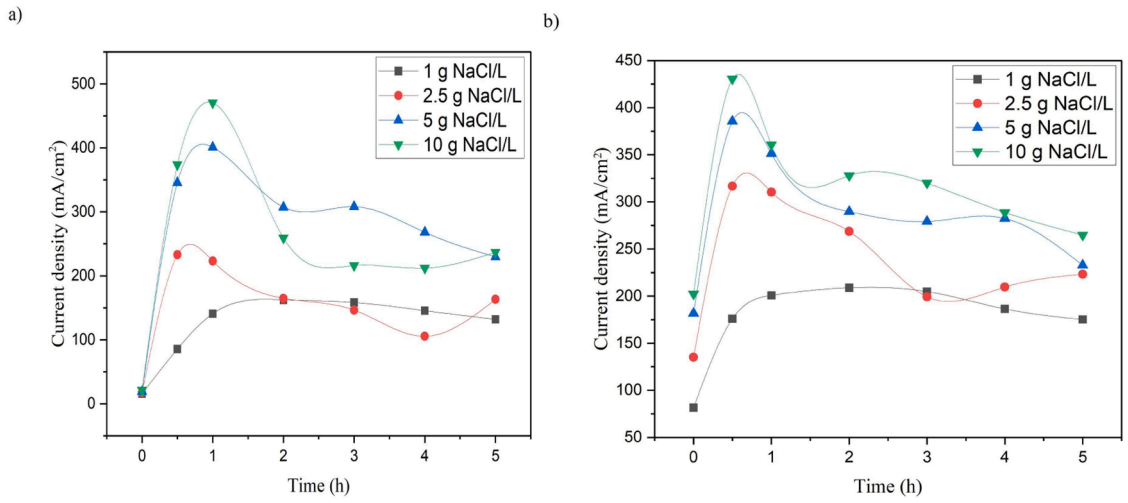

Fig. 10. Variation of current density over time for the reactor without WBCS (a) and when the reactor has WBCS (b).

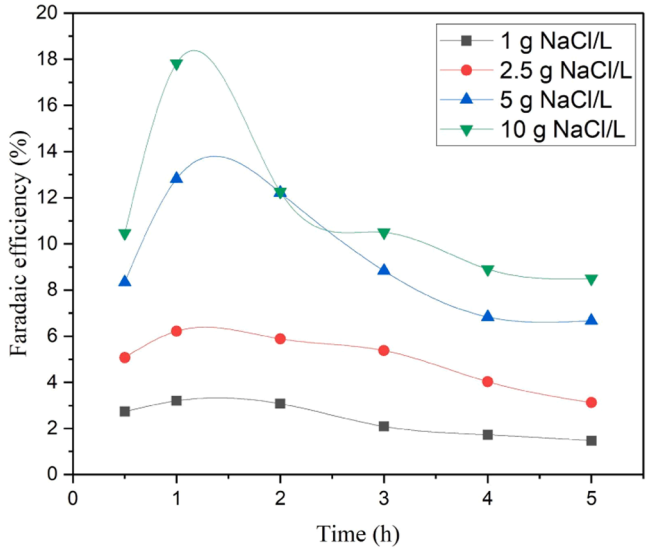

Fig. 11. Faradaic efficiency (%) as a function of NaCl concentration (g/L) and time (h) of the system with WBCS.

corresponding to the precipitated $Cr(OH)_3$. The highly alkaline medium (pH > 10.5) destabilizes the solubility of $Cr(OH)_3$, and it precipitates at short times [47]. Another factor that helps the precipitation is the temperature in the cathodic compartment, which is higher than 90 °C. The $Cr(OH)_3$ solubility decreases by 2.5 orders of magnitude at temperatures higher than 90 °C [48], so the complex and metastable compounds of Cr^{3+} with collagen break down, precipitating as amorphous $Cr(OH)_3$. High concentrations of NaOH exponentially favor alkaline hydrolysis, extracting collagen and precipitating most of the Cr^{3+} as $Cr(OH)_3(OH_2)_3$. Temperatures higher than 60 °C also contribute to Cr^{3+} dehydration, generating amorphous $Cr(OH)_3$ [48] with low solubility ($Kps = 6.7 \times 10^{-3}$), so at pH > 10 most of the $Cr(OH)_3$ precipitates [41].

In summary, the hydrolysis of WBCS by the OH^- generated in the system was due to breaking the chromium-collagen bond, which occurs mainly in the first two hours of the process. Reaction parameters have different effects on the products: at pH < 10.5, partial precipitation of $Cr(OH)_3$ occurs. Increasing the NaCl concentration increases the pH and temperature and decreases the reaction time.

3.3.3. *Influence of current density and faradaic efficiency*

When the concentration of NaCl in the anodic compartments was increased, the presence of Na^+ and Cl^- ions in the system increased, generating significant ion transfer. Therefore, the electric current density varied depending on the NaCl electrolysis at different concentrations. It reached the highest current density for systems without WBCS at 1 h of reaction, then decreased at 2 h, tending to be constant at longer reaction times (Fig. 10a). However, when WBCS was present in the system, the highest electric current density was reached at 0.5 h of reaction and subsequently decreased with reaction time (Fig. 10b). NaOH consumption for WBCS hydrolysis indirectly accelerated the NaCl electrolysis, decreasing by 0.5 h to reach the highest electric current density. Likewise, the increase in electric current density influences the increase in temperature and accelerates the WBCS hydrolysis reaction.

Electrochemical efficiency is proportional to the electrolysis of NaCl and H_2O, which generates OH^- ions for the hydrolysis of WBCS. In this sense, the highest faradaic efficiency occurred at 1 h of reaction and is directly related to the initial NaCl concentration in the system (Fig. 11). Subsequently, the efficiency decreases due to NaCl depletion and reduction of ionic mobility.

The faradaic efficiency for NaCl electrolysis was low, obtaining 12.8 % (5 g NaCl/L) and 17.8 % (10 g NaCl/L), but it was sufficient for the complete hydrolysis of WBCS with OH- to separate Cr^{3+} from collagen, as shown in Table 1. Some consumption of electrical energy supplied through the electrodes was transformed into heat, allowing the reaction system to reach temperatures between 60 and 99 °C.

3.3.4. *Sustainability and circular economy*

The process involves the simultaneous electrolysis of NaCl and hydrolysis of WBCS, where the energy required for the first reaction is used to carry out the second reaction. Furthermore, increasing the NaCl concentration increases the temperature in the cathode compartment for WBCS hydrolysis. The total reaction time is <2 h, and using the NaCl discarded from the hides preservation (zero cost).

Table 2 compares the costs of the hydrolysis process per kg of WBCS treated with H_2SO_4, NaOH, and electrohydrolysis (this work). It is observed that performing two processes in the same step and using NaCl significantly reduces the treatment cost. Regarding the use of the products obtained, the precipitated $Cr(OH)_3$ is acidified with H_2SO_4 to Cr_3+ (pH = 3) and recycled to the tanning process [49]. Bleach (NaClO) could be obtained from the chlorine gas generated in the anode cells as a commercially valuable by-product. The acidic solution from the anode cell would neutralize the basic liming effluent (pH=11–12) in the treatment stage (the mass balance is shown in Section 1). Collagen can be used as a raw material for adhesives [10], fertilizers [50], etc. These characteristics, the reaction conditions, the use of the different compounds obtained, and the cost confer the process sustainability.

Table 2
Cost analysis and efficiency comparison among electro-hydrolysis and conventional hydrolysis.

Process	1st stage. Compound acquisition				2nd stage. Hydrolysis of WBCS				Total Cost (1st + 2nd stage) (Dollars)	Chromium extraction (%)	Product quality	Reference
	Compound	Quantity / Kg of WBSC	Cost (Dollars)	Total 1st stage (Dollars)	Reaction temperature (°C)	Time (hours)	Solution volume / kg of WBSC	Energy (kW/h)	Total 2nd stage (Dollars)			
Acid Hydrolysis	H_2SO_4	0.457 kg	$5.78	$2.75	40	144	10 liters	29	$3.55	$6.29	60	Not reported	21
Basic Hydrolysis	NaOH	0.235 kg	$6.18	$1.45	70	1.5	12.5 liters	0.54	$0.07	$1.52	87	Partially degraded collagen	23
Electrochemical Hydrolysis	NaCl	0.01 kg	$0.62	$0.01	99	1.5	15 liters	1.29	$0.16	$0.16	99	Partially degraded collagen	The present work

4. Conclusions

A technology is presented for separating Cr^{3+} from collagen by electrohydrolysis of WBCS. Two simultaneous reactions occur in the cathodic compartment: the generation of NaOH by NaCl electrolysis and the hydrolysis of WBCS by the OH- ions from NaOH dissociation. Concentrations higher than 5 g of NaCl/L during 1.5 h, reached pH > 10 and temperatures > 90 °C, achieving 99 % separation of Cr^{3+} in the form of precipitated $Cr(OH)_3$, while the collagen solved and remained in solution. The current density varied proportional to NaCl concentration, obtaining the highest faradaic efficiency of 18 % at the reaction time of 1.2 h. This process promotes the circular economy and environmental sustainability in the tanning sector.

CRediT authorship contribution statement

Croswel E. Aguilar Quiroz: Writing – original draft. **Yanet Guevara Ruiz:** Conceptualization. **Javier F. Urquiaga Rios:** Investigation. **Eymi G. Layza Escobar:** Investigation. **Marco A. Siqueira Rodrigues:** Writing – review & editing.

Declaration of competing interest

The authors declare that they have no known competing financial interests or personal relationships that could have appeared to influence the work reported in this paper.

Acknowledgment

This work was partially supported by public resources from CANON VII Project (PIC 04-MOD 1–2023), Universidad Nacional de Trujillo.

This work was developed within the collaboration framework of the Red Economia circular na indústria iberoamericana: resíduos em produtos de valor acrescentado RECIRCULA del CYTED.

Data availability

Data will be made available on request.

References

[1] E.C. Gebremariam, Y.C. Malede, S.V. Prabhu, V. Varadharajan, S. Manivannan, M. Jayakumar, B. Gurunathan, Development of bio-based adhesive using tannery shaving dust: process optimization using statistical and artificial intelligence techniques, Bioresour. Technol. Rep. 22 (2023) 101413, https://doi.org/10.1016/j.biteb.2023.101413.

[2] S. Amdouni, A.B.H. Trabelsi, A.M. Elasmi, R. Chagtmi, K. Haddad, F. Jamaaoui, H. Khedhira, C. Chérif, Tannery fleshing wastes conversion into high value-added biofuels and biochars using pyrolysis process, Fuel 294 (2021) 120423, https://doi.org/10.1016/j.fuel.2021.120423.

[3] C.E.A. Quiroz, E.I.V. Diaz, E.G.L. Escobar, J.F.U. Rios, S.R.J. Rosas, Leaching and heat treatment of chrome shavings: stability of chromium (III), Case Stud. Chem. Environ. Eng. 8 (2023) 100481, https://doi.org/10.1016/j.cscee.2023.100481.

[4] J. Liang, X. Huang, J. Yan, Y. Li, Z. Zhao, Y. Liu, J. Ye, Y. Wei, A review of the formation of Cr(VI) via Cr(III) oxidation in soils and groundwater, Sci. Total. Environ. 774 (2021) 145762, https://doi.org/10.1016/j.scitotenv.2021.145762.

[5] S. Mohanty, A. Benya, S. Hota, M.S. Kumar, S. Singh, Eco-toxicity of hexavalent chromium and its adverse impact on environment and human health in Sukinda Valley of India: a review on pollution and prevention strategies, Environ. Chem. Ecotoxicol. 5 (2023) 46–54, https://doi.org/10.1016/j.enceco.2023.01.002.

[6] P. Majhi, S.M. Samantaray, Effect of hexavalent chromium on paddy crops (Oryza sativa), J. Pharmacogn. Phytochem. 9 (2) (2020) 1301–1305. https://www.phytojournal.com/archives/2020/vol9issue2/PartU/9-2-56-644.pdf.

[7] M.R. Shaibur, Heavy metals in chrome-tanned shaving of the tannery industry are a potential hazard to the environment of Bangladesh, Case Stud. Chem. Environ. Eng. 7 (2022) 100281, https://doi.org/10.1016/j.cscee.2022.100281.

[8] G. Priebe, E. Kipper, A. Gusmão, N. Marcilio, M. Gutterres, Anaerobic digestion of chrome-tanned leather waste for biogas production, J. Clean. Prod. 129 (2016) 410–416, https://doi.org/10.1016/j.jclepro.2016.04.038.

[9] B. Yuan, S. Lai, J. Li, L. Li, S. Bai, Trash into treasure: stiff, thermally insulating and highly conductive carbon aerogels from leather wastes for high-performance electromagnetic interference shielding, J. Mater. Chem. C 9 (7) (2021) 2298–2310, https://doi.org/10.1039/d0tc05480a.

[10] N.E.F. Tapia, H.B. Moina, R. Peñafiel, L.V.P. Aldás, Recycling of collagen from solid tannery waste and prospective utilization as adhesives, F1000Research 13 (2024) 1228, https://doi.org/10.12688/f1000research.155450.1.
[11] M. Ashokkumar, N.T. Narayanan, B.K. Gupta, A.L.M. Reddy, A.P. Singh, S. K. Dhawan, B. Chandrasekaran, D. Rawat, S. Talapatra, P.M. Ajayan, P. Thanikaivelan, Conversion of industrial bio-waste into useful nanomaterials, ACS. Sustain. Chem. Eng. 1 (6) (2013) 619–626, https://doi.org/10.1021/sc3001564.
[12] H.C. Wells, K.H. Sizeland, R.L. Edmonds, W. Aitkenhead, P. Kappen, C. Glover, B. Johannessen, R.G. Haverkamp, Stabilizing chromium from leather waste in biochar, ACS. Sustain. Chem. Eng. 2 (7) (2014) 1864–1870, https://doi.org/10.1021/sc500212r.
[13] M. Velusamy, B. Chakali, S. Ganesan, F. Tinwala, S.S. Venkatachalam, Investigation on pyrolysis and incineration of chrome-tanned solid waste from tanneries for effective treatment and disposal: an experimental study, Environ. Sci. Pollut. Res. 27 (24) (2019) 29778–29790, https://doi.org/10.1007/s11356-019-07025-6.
[14] C. Gomes, J. Piccin, M. Gutterres, Optimizing adsorption parameters in tannery-dye-containing effluent treatment with leather shaving waste, Process Safety Environ. Protec. 99 (2015) 98–106, https://doi.org/10.1016/j.psep.2015.10.013.
[15] M.A. Hashem, M.E.H. Zahin, M.S. Haque, M.S. Milu, M.A. Hasan, S. Payel, Leather shaving dust utilization in brick preparation: solid waste management in tannery, Constr. Build. Mater. 400 (2023) 132769, https://doi.org/10.1016/j.conbuildmat.2023.132769.
[16] E.H. Nashy, O. Osman, A.A. Mahmoud, M. Ibrahim, Molecular spectroscopic study for suggested mechanism of chrome tanned leather, Spectrochim. Acta Part A Molec. Biomolec. Spectrosc. 88 (2011) 171–176, https://doi.org/10.1016/j.saa.2011.12.024.
[17] M.F. Pedrotti, D. Santos, V.H. Cauduro, C.A. Bizzi, E.M. Flores, Ultrasound-assisted extraction of chromium from tanned leather shavings: a promising continuous flow technology for the treatment of solid waste, Ultrason. Sonochem. 89 (2022) 106124, https://doi.org/10.1016/j.ultsonch.2022.106124.
[18] A.S. Popiolski, R.M. Dallago, J. Steffens, M.L. Mignoni, L.D. Venquiaruto, D. Santos, F.A. Duarte, Ultrasound-assisted extraction of Cr from residual tannery leather: feasibility of ethylenediaminetetraacetic acid as the extraction solution, ACS. Omega 3 (11) (2018) 16074–16080, https://doi.org/10.1021/acsomega.8b02241.
[19] S. Famielec, Chromium concentrate recovery from solid tannery waste in a thermal process, Materials. (Basel) 13 (7) (2020) 1533, https://doi.org/10.3390/ma13071533.
[20] A. Malek, M. Hachemi, V. Didier, New approach of depollution of solid chromium leather waste by the use of organic chelates, J. Hazard. Mater. 170 (1) (2009) 156–162, https://doi.org/10.1016/j.jhazmat.2009.04.118.
[21] M.J. Ferreira, M.F. Almeida, S.C. Pinho, I.C. Santos, Finished leather waste chromium acid extraction and anaerobic biodegradation of the products, Waste Manag. 30 (6) (2010) 1091–1100, https://doi.org/10.1016/j.wasman.2009.12.006.
[22] L. Wang, J. Li, Y. Jin, M. Chen, J. Luo, X. Zhu, Y. Zhang, Study on the removal of chromium(III) from leather waste by a two-step method, J. Industr. Eng. Chem. 79 (2019) 172–180, https://doi.org/10.1016/j.jiec.2019.06.030.
[23] J.B. Hinojosa, L.M. Saldaña, Optimization of alkaline hydrolysis of chrome shavings to recover collagen hydrolysate and chromium hydroxide, Leather Footwear J. 20 (1) (2020) 15–28, https://doi.org/10.24264/lfj.20.1.2.
[24] C. Mu, W. Lin, M. Zhang, Q. Zhu, Towards zero discharge of chromium-containing leather waste through improved alkali hydrolysis, Waste Manag. 23 (9) (2003) 835–843, https://doi.org/10.1016/s0956-053x(03)00040-0.
[25] B.M. Tudorel, B.M. Iulia, P. Melinda, Influence of reaction conditions on the Alkaline hydrolysis of Chamois leather Waste, DOAJ (DOAJ: Direct. Open Access J.) (2017). https://doaj.org/article/298c06d4045b41e38f0bdff008a5ad78.
[26] A. Kumar, F. Du, J.H. Lienhard, Caustic soda production, energy efficiency, and electrolyzers, ACS. Energy Lett. 6 (10) (2021) 3563–3566, https://doi.org/10.1021/acsenergylett.1c01827.
[27] S. Savari, S. Sachdeva, A. Kumar, Electrolysis of sodium chloride using composite poly(styrene-co-divinylbenzene) cation exchange membranes, J Memb Sci 310 (1–2) (2007) 246–261, https://doi.org/10.1016/j.memsci.2007.10.049.
[28] O.O. Balayeva, A.A. Azizov, M.B. Muradov, R.M. Alosmanov, G.M. Eyvazova, S. J. Mammadyarova, Cobalt chromium-layered double hydroxide, α- and β- Co(OH)2 and amorphous Cr(OH)3: synthesis, modification and characterization, Heliyon. 5 (11) (2019) e02725, https://doi.org/10.1016/j.heliyon.2019.e02725.
[29] Q. Zhang, Q. Wang, S. Lv, J. Lu, S. Jiang, J.M. Regenstein, L. Lin, Comparison of collagen and gelatin extracted from the skins of Nile tilapia (Oreochromis niloticus) and channel catfish (Ictalurus punctatus), Food Biosci. 13 (2015) 41–48, https://doi.org/10.1016/j.fbio.2015.12.005.
[30] M. Zhang, Z. Li, P. Jiang, T. Lin, X. Li, D. Sun, Characterization and cell response of electrospun Rana chensinensis skin collagen/poly(l-lactide) scaffolds with different fiber orientations, J. Appl. Polym. Sci. 134 (34) (2017), https://doi.org/10.1002/app.45109.
[31] B. León-Mancilla, M. Araiza-Téllez, J. Flores-Flores, M. Piña-Barba, Physico-chemical characterization of collagen scaffolds for tissue engineering, J. Appl. Res. Technol. 14 (1) (2016) 77–85, https://doi.org/10.1016/j.jart.2016.01.001.
[32] H. Xiao, G. Cai, M. Liu, Hydroxyl radical induced structural changes of collagen, J. Spectrosc. 21 (2) (2007) 91–103, https://doi.org/10.1155/2007/496174.
[33] K. Belbachir, R. Noreen, G. Gouspillou, C. Petibois, Collagen types analysis and differentiation by FTIR spectroscopy, Anal. Bioanal. Chem. 395 (3) (2009) 829–837, https://doi.org/10.1007/s00216-009-3019-y.
[34] M. Iafisco, I. Foltran, S. Sabbatini, G. Tosi, N. Roveri, Electrospun nanostructured fibers of collagen-biomimetic apatite on titanium alloy, Bioinorg. Chem. Appl. 2012 (2012) 1–8, https://doi.org/10.1155/2012/123953.
[35] C. Stani, L. Vaccari, E. Mitri, G. Birarda, FTIR investigation of the secondary structure of type I collagen: new insight into the amide III band, Spectrochim. Acta Part A Molec. Biomolec. Spectrosc. 229 (2019) 118006, https://doi.org/10.1016/j.saa.2019.118006.
[36] J. Liu, Z. Zhang, M. Zhang, M.G.A. Kaya, F. Wang, K. Tang, Co-pyrolysis of chrome-tanned leather shavings with wheat straw: thermal behavior, kinetics and pyrolysis products, Energy 301 (2024) 131733, https://doi.org/10.1016/j.energy.2024.131733.
[37] C. Sethuraman, K. Srinivas, G. Sekaran, Pyrolysis coupled pulse oxygen incineration for disposal of hazardous chromium impregnated fine particulate solid waste generated from leather industry, J. Environ. Chem. Eng. 2 (1) (2013) 516–524, https://doi.org/10.1016/j.jece.2013.10.006.
[38] R. Fu, H. Wang, J. Yan, R. Li, B. Wang, C. Jiang, Y. Wang, T. Xu, A cost-effective and high-efficiency online ED-BMED integrated system enables the conversion of 3.5 wt % NaCl aqueous solution into 6.20 mol/L NaOH, Chem. Eng. Sci. 270 (2023) 118523, https://doi.org/10.1016/j.ces.2023.118523.
[39] A. Kumar, K.R. Phillips, G.P. Thiel, U. Schröder, J.H. Lienhard, Direct electrosynthesis of sodium hydroxide and hydrochloric acid from brine streams, Nat. Catal. 2 (2) (2019) 106–113, https://doi.org/10.1038/s41929-018-0218-y.
[40] M. Reig, S. Casas, C. Valderrama, O. Gibert, J. Cortina, Integration of monopolar and bipolar electrodialysis for valorization of seawater reverse osmosis desalination brines: production of strong acid and base, Desalination. 398 (2016) 87–97, https://doi.org/10.1016/j.desal.2016.07.024.
[41] N. Papassiopi, K. Vaxevanidou, C. Christou, E. Karagianni, G. Antipas, Synthesis, characterization and stability of Cr(III) and Fe(III) hydroxides, J. Hazard. Mater. 264 (2013) 490–497, https://doi.org/10.1016/j.jhazmat.2013.09.058.
[42] D. Rai, D.A. Moore, N.J. Hess, K.M. Rosso, L. Rao, S.M. Heald, Chromium(III) hydroxide solubility in the aqueous K+-H+-OH−-CO2-HCO 3 − -CO 3 2− -H2O system: a thermodynamic model, J. Solution. Chem. 36 (10) (2007) 1261–1285, https://doi.org/10.1007/s10953-007-9179-5.
[43] R. Oruko, R. Selvarajan, H. Ogola, J. Edokpayi, J. Odiyo, Contemporary and future direction of chromium tanning and management in sub Saharan Africa tanneries, Process Safety Environ. Protect. 133 (2019) 369–386, https://doi.org/10.1016/j.psep.2019.11.013.
[44] B. Mella, A.C. Glanert, M. Gutterres, Removal of chromium from tanning wastewater and its reuse, Process Safety Environm. Protect. 95 (2015) 195–201, https://doi.org/10.1016/j.psep.2015.03.007.
[45] J. Ma, T. E, S. Yang, L. Chen, Y. Cheng, J. Yu, Y. Li, Stabilizing Cr(III) deriving from tannery sludge with kaolin and organic matter, Environ. Res. 236 (2023) 116798, https://doi.org/10.1016/j.envres.2023.116798.
[46] T. E, Y. Cheng, S. Yang, H. Zou, Recovering Cr(III) from chromium-containing waste: an in-depth study on mechanism via retaining organic matters, J. Environ. Chem. Eng. 9 (5) (2021) 105598, https://doi.org/10.1016/j.jece.2021.105598.
[47] J. Namieśnik, A. Rabajczyk, Speciation analysis of chromium in environmental samples, Crit. Rev. Environ. Sci. Technol. 42 (4) (2011) 327–377, https://doi.org/10.1080/10643389.2010.518517.
[48] D. Rai, B.M. Sass, D.A. Moore, Chromium(III) hydrolysis constants and solubility of chromium(III) hydroxide, Inorg. Chem. 26 (3) (1987) 345–349, https://doi.org/10.1021/ic00250a002.
[49] A. Misganaw, B. Akenaw, S. Getu, Determination of the level of chromium (III) and comparison of chemical precipitating agents to recover and reuse it from tannery waste water, Desalin. Water Treat 317 (2024) 100150, https://doi.org/10.1016/j.dwt.2024.100150.
[50] H. Chen, Y. Li, H. Dai, L. Chen, X. Ding, Z. Hu, Collagen hydrolyzed extract derived from leather waste as a multifunctional additive for the preparation of granular fertilizer, Sustain. Chem. Pharm. 36 (2023) 101327, https://doi.org/10.1016/j.scp.2023.101327.